Continuum spectrum calculations with Explicitly Correlated Gaussians

Exam number: 220124

Supervisor: Dmitri Fedorov

Department of Physics and Astronomy
Aarhus University

August 2026

Preface

The following is a 15 ECTS bachelor thesis written such that a student at the end of their bachelor's degree in physics at Aarhus University should be able to understand it. In particular a general understanding of quantum mechanics, particle physics, and linear algebra for a full understanding.

The thesis is based on a model proposed by my supervisor Dmitri Fedorov, to whom I extent my sincere thanks for his help throughout the creation of this thesis.

Resumé

I dette bachelorprojekt i fysik undersøges det om Eksplicit Korrelerede Gauss funktioner (EKGer) kan bruges til at bestemme massen af $N(1440)$ Roper resonansen ved brug af Kunstigt Begrænsnings Potentiale metoden (KBP). Det brugte potentiale er for en harmonisk oscillator.

Systemet analyseres i Jakobiske koordinater, og energierne til at bestemme Roper resonansen findes ved at minimisere resultatet af et generaliseret egenværdi problem, hvor bassen består af EKGer. Foruden bassen af EKGer er det generaliserede egenværdiproblem konstrueret med en Hamilton, der beskriver interaktionen mellem en bar nukleon og en nukleon beklædt med en pion.

Resultatet af projektet er, at EKGer begrænset af en harmonisk oscillator ikke kan bruges til at bestemme massen af $N(1440)$ Roper resonansen.

Abstract

This bachelor thesis in physics examines if Explicitly Correlated Gaussians (ECGs) can be used to determine the mass of the particle $N(1440)$ Roper resonance using the Artificial Confining Potential method (ACP). The potential used is for a harmonic oscillator.

The system is analysed in Jacobian coordinates and the energies used to determine the Roper resonance are found by minimising the result of a generalised eigenvalue problem where the basis is constructed of ECGs. Besides the basis of ECGs, the generalised eigenvalue problem is constructed with a Hamiltonian describing the interaction between a bare nucleon and a nucleon dressed by a pion.

The result of this thesis is that ECGs confined by a harmonic oscillator cannot be used to determine the mass of $N(1440)$ Roper resonance.

Contents

1 Introduction **1**

2 Theory **2**
2.1 Decay of N(1440) 2
2.2 The nucleon in MEM 2
2.3 Jacobi coordinates 4
2.4 Explicitly Correlated Gaussians 5
2.5 Anti-symmetrisation of the Gaussians 8
2.6 The harmonic oscillator 9
2.7 Avoided crossings 10
2.8 The strength function 10

3 Calculations **13**
3.1 Construction of the ECG matrices 13
3.2 Construction of the ECGs 14
3.3 Analytical calculations of integrals 14
3.4 Degeneracies 19

4 Results **20**
4.1 Varying S_w 20
4.2 Varying b_o 22
4.3 Relativistic approach 23

5 Discussion **24**
5.1 Varying S_w 24
5.2 Varying b_o 26
5.3 Relativistic approach 26
5.4 Change of method 26

6 Conclusion **27**

A Solutions to the sigma and tau overlaps **A**

B Analytical calculation of harmonic oscillator potential integral **C**

C Analytical calculation of strength function integral **E**

D Numerical methods **G**

E Plots with all degenerate states **H**

E.1 S_w as a parameter . . . . . H

E.1.1 The symmetric Gaussian . . . . . H

E.1.2 The anti-symmetric Gaussian . . . . . J

E.2 b_o as the parameter . . . . . M

1 Introduction

In his article *The N(1440) Roper resonance in the nuclear model with explicit mesons* D.V. Fedorov the $N(1440)$ Roper resonance is shown to naturally appear in the nuclear Model with Explicit Mesons (MEM) [1]. In this bachelor thesis the result of said article is attempted recreated while using the popular method of Explicitly Correlated Gaussians (ECGs) [2] with a harmonic oscillator potential as an Artificial Confining Potential (ACP).

The $N(1440)$ Roper resonance, also known as $N(1440)$ or just Roper resonance, is an excited state of the nucleon (proton or neutron) which primarily decays (55%-75%) into a $N\pi$ state [3, 4]. This yields a few-body system which is the reason MEM is utilised. The problem is solvable without ECGs, which is done in [1]. However, the method in [1] can only be used on two-body systems. If ECGs with an ACP can be used to determine the mass of $N(1440)$ it is also very likely, that it can be used on more complex many-body systems.

2 Theory

2.1 Decay of N(1440)

The object of this bachelor thesis is the particle $N(1440)$. $N(1440)$ is an unstable nucleon consisting of either $udd\,(N^0)$ or $uud\,(N^+)$. The primary decay channel of this particle is the $N\pi$ state. However, for the purposes of simplicity only the N^+ state is examined. Though, the N^0-state should yield similar results. Including spin there are four possible decays for the primary decay channel [3].

$$\begin{aligned} N^+ &\to p \uparrow \pi^0, \\ N^+ &\to p \downarrow \pi^0, \\ N^+ &\to n \uparrow \pi^+, \\ N^+ &\to n \downarrow \pi^+. \end{aligned} \tag{2.1}$$

p denotes a proton and n a neutron, which will also be written as:

$$p = \begin{pmatrix} 1 \\ 0 \end{pmatrix}, \; n = \begin{pmatrix} 0 \\ 1 \end{pmatrix}. \tag{2.2}$$

2.2 The nucleon in MEM

The Nuclear Model with Explicit Mesons (MEM) is a model in which nucleons interact by emitting and absorbing mesons. The mesons are treated explicitly. This entails that the mesons are treated similarly to the nucleons [5].

In this thesis the one-pion approximation is used, meaning the nucleon can be in one of two states. Either it is a bare nucleon, or it is a nucleon dressed by one pion. Thus, giving us the following wave-function:

$$\Psi = \begin{pmatrix} \psi_0(\vec{R}) \\ \psi_1(\vec{R}, \vec{r}) \end{pmatrix}. \tag{2.3}$$

With ψ_0 is the state of the bare nucleon, which only depends on the centre of

mass vector ($\vec{R}$) of the system, while ψ_1 is the state of the nucleon with one pion, which depends on both the centre of mass vector and the position of the pion ($\vec{r}$) [1].

The only possible state of ψ_0 must be $|p\uparrow\rangle$ as any other state would violate CP-conservation for the N^+ state.

The Hamiltonian which acts on this wavefunction can be described as:

$$H = \begin{bmatrix} K_{nuc} + m_N & W^\dagger \\ W & K_{nuc} + m_N + K_\pi + m_\pi \end{bmatrix}, \tag{2.4}$$

where K_{nuc} and K_π are kinetic energy operators for the nucleon and the pion respectively. Similarly, m_N and m_π are the masses of the nucleon and the pion. W is the pion emission and absorption operators. As isospin, angular momentum, and parity should be conserved the simplest W-operator can be written as [1]:

$$W = (\vec{\tau}\vec{\pi})(\vec{\sigma}\vec{r})F(r). \tag{2.5}$$

$\vec{\sigma}$ is the vector of Pauli matrices acting on the spin of the nucleon. $\vec{\tau}$ is the isovector of Pauli matrices acting on the isospin of the nucleon. Lastly $F(r)$ is a short-range form factor. $\vec{\tau}\vec{\pi}$ is given as:

$$\vec{\tau}\vec{\pi} = \tau_0\pi^0 + \sqrt{2}\tau_-\pi^+ + \sqrt{2}\tau_+\pi^-, \tag{2.6}$$

with π^0, π^+, π^- being the physical pions and the τ matrices are described as follows:

$$\tau_0 = \begin{pmatrix} 1 & 0 \\ 0 & -1 \end{pmatrix}, \tau_+ = \begin{pmatrix} 0 & 1 \\ 0 & 0 \end{pmatrix}, \tau_- = \begin{pmatrix} 0 & 0 \\ 1 & 0 \end{pmatrix}. \tag{2.7}$$

The basis of Pauli matrices is $\sigma_0, \sigma_+, \sigma_-$ instead of the usual $\sigma_x, \sigma_y, \sigma_z$. These are given by:

$$\sigma_0 = \begin{pmatrix} 1 & 0 \\ 0 & -1 \end{pmatrix}, \sigma_+ = \begin{pmatrix} 0 & 1 \\ 0 & 0 \end{pmatrix}, \sigma_- = \begin{pmatrix} 0 & 0 \\ 1 & 0 \end{pmatrix}. \tag{2.8}$$

The wavefunction is normalised as:

$$\langle\Psi|\Psi\rangle = \langle\psi_0|\psi_0\rangle + \langle\psi_1|\psi_1\rangle = \int_V d^3\,R|\psi_0|^2 + \int_V d^3\,R \int_V d^3\,r|\psi_1|^2 = 1. \quad (2.9)$$

Here V is the normalisation volume. With this in mind the dimension of W must necessarily be $E/\sqrt{V}$. We can therefore describe $F(r)$ as follows:

$$F(r) = S_\omega \exp(-r^2/b_w^2), \quad (2.10)$$

with b_w being a variable which has a unit of length and S_w being a variable strength factor with unit $E/\sqrt{r^5}$.

2.3 Jacobi coordinates

while working with particle systems, it is often advantageous to use Jacobi coordinates instead of relative coordinates, as they are generated recursively and therefore does not change the former coordinates, when a new particle is added. For an N-particle system they are described by the following equation:

$$\mathbf{r}_n = \frac{1}{m_n}\sum_{i=1}^{n} m_i\mathbf{x}_i - \mathbf{x}_{i+1}. \quad (2.11)$$

The last coordinate in the sequence will always be from the point of reference to the systems centre of mass:

$$\mathbf{r}_N = \frac{1}{m_N}\sum_{i=1}^{N} m_i\mathbf{x}_i, \quad (2.12)$$

with

$$m_n = \sum_{i=1}^{n} m_i, \quad (2.13)$$

and $\mathbf{x}_i$ being the coordinates for the particles from the point of reference.

We can describe the transformation from a normal coordinate system to the Jacobi coordinates by a matrix such that $\mathbf{r} \to J\mathbf{r}$ [6]:

$$J = \begin{pmatrix} 1 & -1 & 0 & \cdots & 0 \\ \frac{m_1}{\sum_{i=1}^{2} m_i} & \frac{m_2}{\sum_{i=1}^{2} m_i} & -1 & \cdots & 0 \\ \vdots & \vdots & \vdots & \ddots & \vdots \\ \frac{m_1}{\sum_{i=1}^{N-1}} & \frac{m_2}{\sum_{i=1}^{N-1}} & \cdots & \cdots & -1 \\ \frac{m_1}{\sum_{i=1}^{N}} & \frac{m_2}{\sum_{i=1}^{N}} & \cdots & \cdots & \frac{m_N}{\sum_{i=1}^{N}} \end{pmatrix} \tag{2.14}$$

As there will not be any external forces on the system used, the centre-of-mass is used as the frame of reference. And it can conveniently be chosen to have position **0**. This makes the last coordinate zero and the problem is then reduced to an N-1 problem instead of an N problem.

For the bare nucleon state the centre-of-mass is simply the nucleon and therefore the kinetic energy of the bare nucleon will always be zero.

2.4 Explicitly Correlated Gaussians

Explicitly Correlated Gaussians (ECG) is a method developed to describe N-particle wave function by using a basis of Gaussian functions. This is possible due to the variational principle, which states [2]:

$$\frac{\langle \Psi | H | \Psi \rangle}{\langle \Psi | \Psi \rangle} \geq E_{exact}. \tag{2.15}$$

All constructed wavefunctions can therefore be used to determine an upper bound for the energy. Using Gaussians is advantageous due to the simplicity of the function thus making it especially useful for numerical calculations.

When using the ECG method, the following Gaussian is usually used:

$$\Psi = \exp\left(-\sum_{i,j}^{N} A_{ij} \mathbf{r}_i \cdot \mathbf{r}_j \right) = \exp(-\mathbf{r}^{\mathbf{T}} A \mathbf{r}), \tag{2.16}$$

where A_{ij} are adjustable parameters, described by the matrix in eq. 2.20. N is the number of used Gaussians. $\mathbf{r}$ is a vector of size N of spatial coordinate vectors. However, it can be, and is in this case, useful to include a shift of the coordinates, which is written as follows:

$$\Psi = \exp(-(\mathbf{r}-\mathbf{s})^{\mathbf{T}} A(\mathbf{r}-\mathbf{s})) = \exp(-\mathbf{r}^{\mathbf{T}} A\mathbf{r} - \mathbf{s}^{\mathbf{T}} A\mathbf{s} + 2\mathbf{s}^{\mathbf{T}} A\mathbf{r}). \tag{2.17}$$

$\mathbf{s}$ is the shift. Furthermore, as $\mathbf{s}^{\mathbf{T}} A\mathbf{s}$ does not depend on $\mathbf{r}$ it can simply be ignored. To simplify the notation the factor of $2A\mathbf{s}$ is defined as $\mathbf{a}$.

$$\mathbf{a} = 2A\mathbf{s}. \tag{2.18}$$

Thus, the ECGs to be used in the calculations can simply be written as:

$$\Psi = \exp(-\mathbf{r}^{\mathbf{T}} A\mathbf{r} + \mathbf{a}^{\mathbf{T}}\mathbf{r}). \tag{2.19}$$

The matrix A is a symmetric positive-definite matrix, meaning $A_{ij} = A_{ji}$ and all eigenvalues of A must be positive. It can be described by:

$$A = \sum_{i<j=1}^{N} \frac{w_{ij} w_{ij}^{\mathbf{T}}}{b_{ij}^2}. \tag{2.20}$$

Here w_{ij} is a vector of size N with the i'th element being 1 and the j'th element being -1. Therefore, for a three-body system[1] these will be described as:

$$w_{12} = \begin{pmatrix} 1 \\ -1 \\ 0 \end{pmatrix}, \quad w_{13} = \begin{pmatrix} 1 \\ 0 \\ -1 \end{pmatrix}, \quad w_{23} = \begin{pmatrix} 0 \\ 1 \\ -1 \end{pmatrix}. \tag{2.21}$$

[1]While a three-body system is not actually used for the calculations it is used as the example. This is done because it is easier to show the general construction with a three-body system as opposed to a two- or one-body system.

w_i can be described similarly. However, these do not include the -1 element. For a three-body system the w_i vectors are as follows:

$$w_1 = \begin{pmatrix} 1 \\ 0 \\ 0 \end{pmatrix}, \quad w_2 = \begin{pmatrix} 0 \\ 1 \\ 0 \end{pmatrix}, \quad w_3 = \begin{pmatrix} 0 \\ 0 \\ 1 \end{pmatrix}. \tag{2.22}$$

When transforming the w_{ij} vectors into Jacobi coordinates, it can be described with the U-matrix $U = J^{-1}$ as $w_{ij} \rightarrow U^T w_{ij}$. In the system where the centre of mass coordinate is removed the last column is removed.

If eq. 2.20 is used in eq. 2.19 the sum will now be described as:

$$\begin{aligned} -\mathbf{r^T} A \mathbf{r} = -\mathbf{r^T} \sum_{i<j}^{N} \frac{w_{ij} w_{ij}^{\mathbf{T}}}{b_{ij}^2} \mathbf{r} &= -\sum_{i<j}^{N} \frac{(\mathbf{r^T} w_{ij})(w_{ij}^{\mathbf{T}} \mathbf{r})}{b_{ij}^2} \\ &= -\sum_{i<j}^{N} \frac{(\mathbf{r}_i - \mathbf{r}_j)^2}{b_{ij}^2}. \end{aligned} \tag{2.23}$$

The wavefunction can be further improved for calculations by using multiple Gaussians, thus changing the wavefunction to:

$$\psi = \sum_{i=1}^{N} c_i e^{-\mathbf{r^T} A_i \mathbf{r} + \mathbf{a}_i^{\mathbf{T}} \mathbf{r}}. \tag{2.24}$$

With N being the number of Gaussians used to describe the system and c_i, A_i being variational parameters. A_i is varied by changing the parameter b_{ij}. c_i is found by solving the generalised eigenvalue problem, which is described as [5]:

$$\mathcal{H} c = E \mathcal{N} c. \tag{2.25}$$

$\mathcal{H}$ is obtained by applying the wavefunction (eq. 2.3) onto the Hamiltonian (eq. 2.4) which when also placing the bare nucleon in the centre-of-mass system gives:

$$\mathcal{H} = \langle\Psi|H|\Psi\rangle = \begin{pmatrix} \langle\psi_{0,i}|m_N|\psi_{0,j}\rangle & \langle\psi_{0,i}|W^\dagger|\psi_{1,j}\rangle \\ \langle\psi_{1,i}|W|\psi_{0,j}\rangle & \langle\psi_{1,i}|K_{nuc} + m_N + K_\pi + m_\pi|\psi_{1,j}\rangle \end{pmatrix}. \tag{2.26}$$

$\mathcal{N}$ is the overlap matrix which is described by:

$$\mathcal{N} = \begin{pmatrix} \langle\psi_{0,i}|\psi_{0,j}\rangle & 0 \\ 0 & \langle\psi_{1,i}|\psi_{1,j}\rangle \end{pmatrix}. \tag{2.27}$$

In these equations the notation of $\psi_{n,i}$ and $\psi_{n,j}$ is to show that all entries (Gaussians) of the left wavefunctions should be applied to all entries of the right wavefunctions.

The description of the ECG sum has been simplified above, where it simply is a description of the Gaussians. When describing a physical system, it is necessary to add a physical state to each Gaussian. In this case this physical state is described by $|\text{nuc}\,, \text{spin}\,, \text{pion}\rangle$ with nuc being a nucleon (either proton or neutron), spin being either spin up or spin down, and the pion being either $\pi^+, \pi^-,$ or π^0. For ψ_1 it will therefore look like this:

$$\begin{aligned} \psi_1 = &\sum_{i=1}^{N} c_i^{p\uparrow\pi^0} G_i^{p\uparrow\pi^0} \,|p\uparrow\pi^0\rangle + \sum_{j=1}^{M} c_j^{p\downarrow\pi^0} G_j^{p\downarrow\pi^0} \,|p\downarrow\pi^0\rangle + \\ &\sum_{k=1}^{L} c_k^{n\uparrow\pi^+} G_k^{n\uparrow\pi^+} \,|n\uparrow\pi^+\rangle + \sum_{h=1}^{F} c_h^{n\downarrow\pi^+} G_h^{n\downarrow\pi^+} \,|n\downarrow\pi^+\rangle\,. \end{aligned} \tag{2.28}$$

Where G describes a Gaussian factor.

2.5 Anti-symmetrisation of the Gaussians

As the parity must be conserved and the pion has parity of -1 [3] the ψ_1 wavefunction needs to be anti-symmetric. Therefore, the Gaussians are described as follows:

$$\begin{aligned} G^{\pi} &= e^{-\mathbf{r}^{\mathbf{T}}A\mathbf{r}+\mathbf{a}^{\mathbf{T}}\mathbf{r}} - e^{-(-\mathbf{r})^{\mathbf{T}}A(-\mathbf{r})+\mathbf{a}^{\mathbf{T}}(-\mathbf{r})} \\ &= e^{-\mathbf{r}^{\mathbf{T}}A\mathbf{r}+\mathbf{a}^{\mathbf{T}}\mathbf{r}} - e^{-\mathbf{r}^{\mathbf{T}}A\mathbf{r}-\mathbf{a}^{\mathbf{T}}\mathbf{r}}. \end{aligned} \tag{2.29}$$

Where A and $\mathbf{a}$ are as described above. When making doing anti-symmetrisation a factor of $1/\sqrt{2}$ appears. However, these factors can simply be included in the c factors.

2.6 The harmonic oscillator

The harmonic oscillator potential is used as an artificial confining potential to limit the possible energies of the system. It is a very common potential used in quantum- and particle-physics. The potential is simply given as [7]:

$$V_o(r) = \frac{1}{2}m_0\omega^2 r^2. \tag{2.30}$$

This potential can be rewritten with $\omega = \frac{\hbar}{m_0 b_0^2}$:

$$V_o(r) = \frac{\hbar^2}{2m_0 b_o^2}\left(\frac{r}{b_o}\right)^2. \tag{2.31}$$

With m_0 being the reduced mass of the system ($m_0 = \frac{m_1 m_2}{m_1+m_2}$) and b_o being a parameter of unit length. The general solution to this potential in three dimensions is [7]:

$$E_N = (N+\frac{3}{2})\hbar\omega = (N+\frac{3}{2})\frac{\hbar^2}{2m_0 b_o^2}. \tag{2.32}$$

However, for the anti-symmetric problem N must be odd, which can be described by $N^{anti-symmetric} = 2n+1$ which yields the following:

$$E_n^{anti-symmetric} = \hbar\omega(2n+\frac{5}{2}) = (2n+\frac{5}{2})\frac{\hbar^2}{2m_0 b_o^2}. \tag{2.33}$$

Similarly, the energy can be found for the symmetric case where $N^{symmetric} = 2n$ which gives a final energy of:

$$E_n^{symmetric} = \hbar\omega(2n + \frac{3}{2}) = (2n + \frac{3}{2})\frac{\hbar^2}{2m_0 b_o^2}. \tag{2.34}$$

The harmonic oscillator potential is added to the generalised eigenvalue problem, such that the Hamiltonian becomes:

$$\mathcal{H} = \begin{pmatrix} \langle\psi_{0,i}|m_N|\psi_{0,j}\rangle & \langle\psi_{0,i}|W^\dagger|\psi_{1,j}\rangle \\ \langle\psi_{1,i}|W|\psi_{0,j}\rangle & \langle\psi_{1,i}|K_{nuc} + m_N + K_\pi + m_\pi + V_o|\psi_{1,j}\rangle \end{pmatrix}. \tag{2.35}$$

2.7 Avoided crossings

Avoided crossings describe the phenomenon where the energies of a quantum system depending on continuous real parameters cannot become equal in value and therefore *cross* each other [8]. Thus, if there is a *crossing* it will show, that the results are wrong.

Furthermore, the avoided crossings plot can also be used to estimate the mass. This is possible, as the energy as a function of the continuous parameter[2] should have a kink, then become near constant until another kink will have it follow the original trajectory. It is this flat part which should be at the resonance energy as shown in [9].

2.8 The strength function

To determine the mass more precisely it can be approximated through the reaction cross-section with a Breit-Wigner shape. It is therefore advantageous to consider a reaction from the ground state to an excited state for the nucleon by the operator $\hat{X}$. The amplitude of this transition is given by the Born approximation through the matrix element [1]:

[2]For the purpose of this thesis the parameter will be b_o from the harmonic oscillator.

$$M_{i\leftarrow 0} = \langle \Psi_i | \hat{X} | \Psi_0 \rangle \,. \tag{2.36}$$

The resonance should not depend on how the excited state is populated, thus making the form of operator $\hat{X}$ unimportant, so long as the matrix element does not become zero. The operator can thus be chosen to be $\hat{X} = \frac{1}{r}$ as experimentation shows $\frac{1}{r^2}$ produces an advantageous strength function [1]. $\frac{1}{r}$ is chosen instead of $\frac{1}{r^2}$ to ensure that the matrix element can be calculated through analytical methods. This results in the following matrix element:

$$M_{i\leftarrow 0} = \int_{-\infty}^{\infty} u_i(r) \frac{1}{r} u_0(r) \, d^3r. \tag{2.37}$$

Where u_i is the sum of Gaussians of the i'th energy level found by the generalised eigenvalue problem. This integral can be calculated analytically, when taking the 1-dimensional system into account.

The discretised version of the strength function is described by [1]:

$$S(E_i) = \frac{1}{\Delta E_1} |M_{i\leftarrow 0}|^2. \tag{2.38}$$

Here $\Delta E_i = E_{i+1} - E_i$, which is the energy difference between the levels in the harmonic oscillator. Utilising the strength function, it is possible to determine the parameters of mass and the width by utilising the Breit-Wigner fit. As the threshold energy is close to the broad Roper resonance it is necessary to use an energy-dependent width [1]. In this case the following definition can be used [10]:

$$S(E) = \frac{2E}{\pi} \frac{\sqrt{E^2 - E_{th}^2}\tilde{\Gamma}}{(E^2 - M^2)^2 + (\sqrt{E^2 - E_{th}^2}\tilde{\Gamma})^2} \theta(E - E_{th}). \tag{2.39}$$

With $\tilde{\Gamma} = \frac{\Gamma M}{\sqrt{M^2 - E_{th}^2}}$. E_{th} is the threshold energy, which for a two-particle decay is simply defined as $E_{th} = m_1 + m_2$, where m_1 and m_2 are the rest masses of

the produced particles. M is the particle mass, Γ is the decay width, and θ is the step function which is defined as:

$$\theta = \begin{cases} 1 & \text{for } r \geq 0 \\ 0 & \text{for } r < 0 \end{cases} \tag{2.40}$$

3 Calculations

The goal of these calculations is solving the generalised eigenvalue problem of eq. 2.25. It is therefore necessary to calculate an array of integrals and construct the ECGs before results can be obtained.

In the following calculations the notation of $c = 1$ is used.

3.1 Construction of the ECG matrices

As defined in eq. 2.3 the total wavefunction is constructed of one one-particle and one two-particle system. For the one-particle there will be no Gaussians, as only the centre-of-mass particle exists. Therefore, it will simply be described with $|p\uparrow\rangle$ as $A = 0$ and $\mathbf{a} = \mathbf{0}$.

For the two-particle system the Jacobian matrix will be:

$$J_2 = \begin{pmatrix} 1 & -1 \\ \frac{m_1}{m_1+m_2} & \frac{m_2}{m_1+m_2} \end{pmatrix}, \tag{3.1}$$

to simplify the calculations, the centre-of-mass coordinate is removed which gives:

$$J_2^{reduced} = \begin{pmatrix} 1 & -1 \end{pmatrix}. \tag{3.2}$$

The inverse of J_2 is:

$$U_2 = \begin{pmatrix} \frac{m_2}{m_1+m_2} & 1 \\ -\frac{m_1}{m_1+m_2} & 1 \end{pmatrix}. \tag{3.3}$$

When reducing U the last column is removed and becomes:

$$U_2^{reduced} = \begin{pmatrix} \frac{m_2}{m_1+m_2} \\ -\frac{m_1}{m_1+m_2} \end{pmatrix}. \tag{3.4}$$

For the two-particle system w is: $w_{12} = \begin{pmatrix} 1 \\ -1 \end{pmatrix}$ The transformation then becomes:

$$w_{12}^{trans} = U^{\mathbf{T}} w_{12} = \begin{pmatrix} \frac{m_2}{m_1+m_2} & -\frac{m_1}{m_1+m_2} \end{pmatrix} \begin{pmatrix} 1 \\ -1 \end{pmatrix} = \begin{pmatrix} 1 \end{pmatrix}. \tag{3.5}$$

The A matrix will now only have one entry, which simplifies calculations:

$$A_2 = \left(\frac{w_{12}^{trans} (w_{12}^{trans})^{\mathbf{T}}}{b^2} \right) = \left(\frac{1}{b^2} \right) \tag{3.6}$$

3.2 Construction of the ECGs

After the construction of the ECG matrices the actual ECGs should be constructed. To construct the bare nucleon, the wavefunction ψ_0 will be as follows:

$$\psi_0 = |p \uparrow\rangle \tag{3.7}$$

ψ_1 is constructed as in eq. 2.29. When doing calculation with those wavefunctions it is important to note that p and n are orthogonal and normalised thus $\langle p|p\rangle = \langle n|n\rangle = 1$ and $\langle p|n\rangle = \langle n|p\rangle = 0$. The same is true for $\uparrow$ and $\downarrow$ and it is also true for π^0, π^+, and π^-.

3.3 Analytical calculations of integrals

The overlap $\langle B, \mathbf{b}|A, \mathbf{a}\rangle$, which is also denoted as M, of shifted Gaussians can be described by an integral. The notation A, B describes the Gaussian matrices as in eq. 2.20 and $\mathbf{a}, \mathbf{b}$ is the shift as defined in eq. 2.18.

$$\begin{aligned} M = \langle B, \mathbf{b}|A, \mathbf{a}\rangle &= \int_0^\infty \exp(-\mathbf{r}^{\mathbf{T}} B \mathbf{r} + \mathbf{b}^{\mathbf{T}} \mathbf{r}) \exp(-\mathbf{r}^{\mathbf{T}} A \mathbf{r} + \mathbf{a}^{\mathbf{T}} \mathbf{r})\, d\mathbf{r}^3 \\ &= \int_0^\infty \exp(-\mathbf{r}^{\mathbf{T}} (B + A) \mathbf{r} + (\mathbf{b} + \mathbf{a})^{\mathbf{T}} \mathbf{r})\, d\mathbf{r}^3. \end{aligned} \tag{3.8}$$

This integral has been calculated in [11] to be:

$$\langle B, \mathbf{b}|A, \mathbf{a}\rangle = e^{\frac{1}{4}\mathbf{v}^{\mathbf{T}}R\mathbf{v}} \left(\frac{\pi^N}{\det(A+B)}\right)^{3/2}, \tag{3.9}$$

where $\mathbf{v} = \mathbf{a} + \mathbf{b}$, $N = \dim(A)$, and $R = (A+B)^{-1}$.

This overlap can be used for any $\langle B, \mathbf{b}|f|A, \mathbf{a}\rangle$, where f does not depend on $\mathbf{r}$. It is therefore necessary to calculate $\langle B, \mathbf{b}|K|A, \mathbf{a}\rangle$, $\langle B, \mathbf{b}|V|A, \mathbf{a}\rangle$, and $\langle B, \mathbf{b}|W|A, \mathbf{a}\rangle$.

The kinetic energy function

Non-relativistic kinetic energy

The non-relativistic kinetic energy operator can be described by:

$$K_{non-rel} = \frac{\hbar^2}{2m}(\mu^{\mathbf{T}}\hat{\mathbf{k}})^2. \tag{3.10}$$

The calculation of this overlap has been done by D.V. Fedorov and is [12]:

$$\begin{aligned} &\langle B, \mathbf{b}|\frac{\hbar^2}{2m}(\mu^{\mathbf{T}}\hat{\mathbf{k}})^2|A, \mathbf{a}\rangle \\ &= \frac{\hbar^2}{2m}\langle B, \mathbf{b}|A, \mathbf{a}\rangle \left(\frac{3}{2\gamma} - \eta^2\right). \end{aligned} \tag{3.11}$$

With γ given by:

$$\frac{1}{\gamma} = 4\mu^{\mathbf{T}}ARB\mu, \tag{3.12}$$

and with $R = (A+B)^{-1}$. In Jacobian coordinate μ is simply 1 or -1 for the 2-body system. Therefore $\mu^{\mathbf{T}}\mu = 1$. η is given by:

$$\vec{\eta} = \mu^{\mathbf{T}}(AR\mathbf{b} - BR\mathbf{a}). \tag{3.13}$$

As the results includes η^2 the μ factor in η can be ignored.

Relativstis kinetic energy

The relativistic kinetic energy operator including the mass operator can be described by:

$$K_{rel} = \sqrt{\hbar^2(\mu^{\mathbf{T}}\hat{\mathbf{k}})^2 + m^2}. \tag{3.14}$$

As the mass is included in the kinetic energy term, it is removed from the $\langle\psi_1|H_{11}|\psi_1\rangle$ entry of the generalised eigenvalue problem.

The calculation of this overlap has been done by D.V. Fedorov and is [12]:

$$\begin{aligned}&\langle B,\mathbf{b}|\sqrt{\hbar^2(\mu^{\mathbf{T}}\hat{\mathbf{k}}) + m^2}|A,\mathbf{a}\rangle \\ &= \langle B,\mathbf{b}|A,\mathbf{a}\rangle \left(\frac{\gamma}{\pi}\right)^{\frac{3}{2}} 2\pi\frac{e^{\gamma\eta^2}}{\gamma\eta}\int_0^\infty x e^{-\gamma x^2}\sqrt{\hbar^2x^2+m^2}\sin(2\gamma\eta x)\,dx.\end{aligned} \tag{3.15}$$

The remaining integral is calculated numerically. In the solution above the sign of η and therefore μ is included twice and μ can thus be ignored.

The harmonic oscillator function

The calculation of $\langle B,\mathbf{b}|V|A,\mathbf{a}\rangle$ is done as follows:

$$\begin{aligned}\langle B,\mathbf{b}|V|A,\mathbf{a}\rangle &= \langle B,\mathbf{b}|\frac{\hbar^2}{2m_0b_o^2}\left(\frac{r}{b_o}\right)^2|A,\mathbf{a}\rangle \\ &= \frac{\hbar^2}{2m_0b_o^4}\langle B,\mathbf{b}|r^2|A,\mathbf{a}\rangle\,.\end{aligned} \tag{3.16}$$

In the two-particle system this problem can be simplified to be:

$$\begin{aligned}\langle B,\mathbf{b}|V|A,\mathbf{a}\rangle &= \frac{\hbar^2}{2m_0b_o^4}\int_{-\infty}^{\infty} e^{-Br^2+\vec{b}\cdot\vec{r}}r^2e^{-Ar^2+\vec{a}\cdot\vec{r}}\,d^3r \\ &= \frac{\hbar^2}{2m_0b_o^4}\int_{-\infty}^{\infty} e^{-\alpha r^2+\vec{\beta}\cdot\vec{r}}r^2\,d^3r.\end{aligned} \tag{3.17}$$

The change of notation from $R^{-1} \to \alpha$ and $\mathbf{v} \to \vec{\beta}$ is done to show that it is no longer the general case, but instead simply the two-particle system. The integral is solved analytically in appendix B, with the result:

$$\langle B, \mathbf{b}|V|A, \mathbf{a}\rangle = \frac{\hbar^2}{2m_0 b_o^4} e^{\frac{\beta^2}{4\alpha}} \left(\frac{\pi}{\alpha}\right)^{3/2} \left(\frac{\beta^2}{4\alpha^2} + \frac{3}{2\alpha}\right). \tag{3.18}$$

The interaction function

The calculation of $\langle B, \mathbf{b}|W|A, \mathbf{a}\rangle$ is done as follows: First it is noted that there are four possible spin systems, these being $\langle\uparrow|\uparrow\rangle$, $\langle\downarrow|\uparrow\rangle$, $\langle\uparrow|\downarrow\rangle$, $\langle\downarrow|\downarrow\rangle$. In the case of a one- or two-particle system the A- and B-matrices become one-dimensional. In this case $\vec{r}$ becomes $w^{\mathbf{T}}r$. Then the calculation can be written as:

$$\begin{aligned}\langle B, \mathbf{b}|W|A, \mathbf{a}\rangle &= \langle B, \mathbf{b}, S_1, N_2, \pi_2|(\vec{\tau}\vec{\pi})(\vec{\sigma}\vec{r})S_w e^{r^2/b_w^2}|A, \mathbf{a}, S_2, N_2, \pi_2\rangle \\ &= \langle N_1, \pi_1|(\vec{\tau}\vec{\pi})|N_2, \pi_2\rangle\, S_w\, \langle B, \mathbf{b}, S_1|\vec{\sigma}(w^{\mathbf{T}}r)e^{r^2/b_w^2}|A, \mathbf{a}, S_2\rangle\,.\end{aligned} \tag{3.19}$$

Here S_1 and S_2 denotes spins states, N_1 and N_2 denotes a nucleon state, and π_1 and π_2 denotes a pion state. Furthermore, as the calculations are done with an additional Gaussian e^{r^2/b_w^2}, which can simply be absorbed in either of the other Gaussians b_{ij} factors, thus making it negligible for the purposes of analytically calculating the integral.

$$\begin{aligned}\langle B, \mathbf{b}, S_1|W|S_2, A, \mathbf{a}\rangle &= \langle N_1, \pi_1|(\vec{\tau}\vec{\pi})|N_2, \pi_2\rangle\, S_w\, \langle B, \mathbf{b}, S_1|\vec{\sigma}(w^{\mathbf{T}}r)|S_2, A', \mathbf{a}\rangle \\ &= \langle N_1, \pi_1|(\vec{\tau}\vec{\pi})|N_2, \pi_2\rangle\, S_w\, \langle S_1|\vec{\sigma}|S_2\rangle\, \langle B, \mathbf{b}|(w^{\mathbf{T}}r)|A', \mathbf{a}\rangle\,.\end{aligned} \tag{3.20}$$

Here A' is used to denote that it has absorbed e^{r^2/b_w^2}. The calculation of $\langle B, \mathbf{b}|(w^{\mathbf{T}}\vec{r})|A, \mathbf{a}\rangle$ is known to yield [13]:

$$\langle B, \mathbf{b}|(w^{\mathbf{T}}\vec{r})|A, \mathbf{a}\rangle = \frac{1}{2} w^{\mathbf{T}} R(\mathbf{a} + \mathbf{b}) M. \tag{3.21}$$

With R and M following the same descriptions as earlier. In the one-dimensional system $w^{\mathbf{T}} = w_1$ The calculations of $\langle S_1|\vec{\sigma}\vec{r}|S_2\rangle$ are found in appendix A and yields the following:

$$\begin{aligned}\langle\uparrow|\vec{\sigma}\vec{r}|\uparrow\rangle = \langle\uparrow|(\vec{\sigma}\vec{r})^\dagger|\uparrow\rangle = r^0,\\ \langle\downarrow|\vec{\sigma}\vec{r}|\uparrow\rangle = \langle\uparrow|(\vec{\sigma}\vec{r})^\dagger|\downarrow\rangle = \sqrt{2}r^+,\\ \langle\downarrow|\vec{\sigma}\vec{r}|\downarrow\rangle = \langle\downarrow|(\vec{\sigma}\vec{r})^\dagger|\downarrow\rangle = -r^0,\\ \langle\uparrow|\vec{\sigma}\vec{r}|\downarrow\rangle = \langle\downarrow|(\vec{\sigma}\vec{r})^\dagger|\uparrow\rangle = \sqrt{2}r^-.\end{aligned} \tag{3.22}$$

The $\vec{\tau}\vec{\pi}$ brakets can also be found in appendix A and are:

$$\begin{aligned}\langle p\pi^0|(\vec{\tau}\vec{\pi})^\dagger|p\rangle = \langle p|\vec{\tau}\vec{\pi}|p\pi^0\rangle = 1\\ \langle n\pi^+|(\vec{\tau}\vec{\pi})^\dagger|p\rangle = \langle p|\vec{\tau}\vec{\pi}|n\pi^+\rangle = \sqrt{2}\end{aligned} \tag{3.23}$$

The strength function integral

For the purposes of constructing the strength function it is necessary to calculate the integral $\int_0^\infty u_i(r)\frac{1}{r^1}u_0(r)\,dr$. $u_i(r)$ and $u_0(r)$ are sums of Gaussians, which for the 2-particle system can be simplified to be:

$$M_{i\leftarrow 0} = \sum_{n=0}^{N_i}\sum_{k=0}^{N_0} C_{i,n}C_{0,k}\int_{-\infty}^{\infty} e^{-r^2A_{i,n}+\vec{a}_{i,n}\vec{r}}\frac{1}{r}e^{-r^2A_{0,k}+\vec{a}_{0,k}\vec{r}}\,d^3r. \tag{3.24}$$

This is simply a sum of integrals on the form:

$$J = \int_{-\infty}^{\infty} e^{-r^2\alpha+\vec{\beta}\vec{r}}\frac{1}{r}\,d^3r. \tag{3.25}$$

Where the notation is the same as the one used with the harmonic oscillator calculations. The calculation of this integral is done in appendix C, and it becomes:

$$J = e^{\frac{\beta^2}{4\alpha}}\frac{2\pi^{3/2}}{\alpha}\,\mathrm{erf}(\frac{\beta}{2\sqrt{\alpha}}). \tag{3.26}$$

Where the error function is calculated numerically.

3.4 Degeneracies

The expected degeneracy of the ground state is one. However, for the excited states the degeneracies of the systems are the expected number of spatial degeneracies times four, which is the number of spin-isospin states. The number of spatial degeneracies are given as [7]:

$$D(N)_{spatial} = \frac{(N+1)(N+2)}{2}. \tag{3.27}$$

Then the total degeneracy is:

$$D(N) = 2(N+1)(N+2). \tag{3.28}$$

For the anti-symmetric states $N = 2n + 1$, which gives the following number of degenerate states:

$$D^{anti-symmetric} = 12, 40, 84, \ldots. \tag{3.29}$$

For the symmetric states $N = 2n$, which gives the following number of degeneracies:

$$D^{symmetric} = 4, 24, 60, \ldots. \tag{3.30}$$

4 Results

The results are obtained by numerically minimising the eigenvalues of eq. 2.35. The minimisation is done through optimisation of the b_{ij} and $\mathbf{s}$ parameters. The numerical method used is further described in appendix D.

4.1 Varying S_w

Firstly, the results are obtained for the non-relativistic system where S_w is varied and symmetric Gaussians are used. This is plotted in figure 1 It is expected, that the energy does not change as the solution to the interaction function is directly proportional to the shift and thus $\langle 0, \mathbf{0}|W|A, \mathbf{a}\rangle + \langle 0, \mathbf{0}|W|A, -\mathbf{a}\rangle = 0$.

The parameters used for these results are $b_o = 2fm$ and $b_w = 1fm$. These parameters are chosen to ensure the oscillator and interaction function respectively would have an impact, while at the same time not making their impacts dominate too much. Furthermore, these parameters are successful when doing the optimisation.

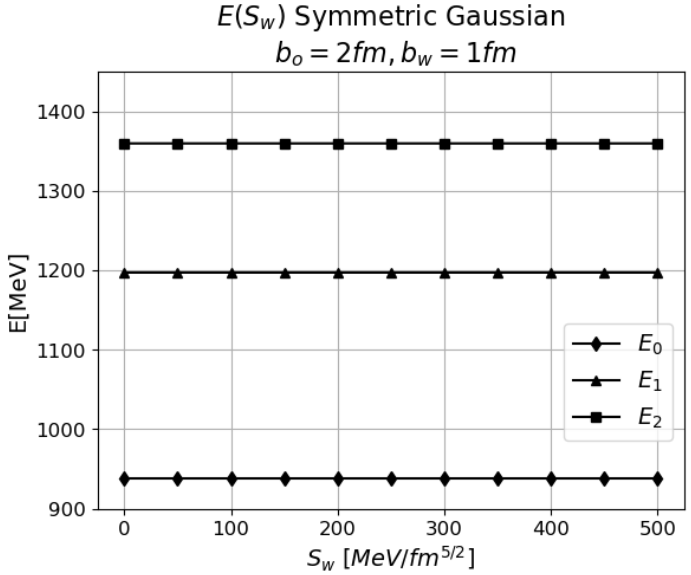

Figure 1: The energy levels as a function of S_w using a symmetric Gaussian on the generalised eigenvalue problem. The parameters used are $b_o = 2$ and $b_w = 1.2$. Only one degeneracy is plotted for each energy level, the remaining degeneracies can be found in appendix E.

For each energy level besides the ground state, degeneracies are expected. However, to simplify the plots only one degeneracy per energy level has been included for the symmetric state. The spectrums with all degeneracies can be found in appendix E.

The results are also obtained with anti-symmetric Gaussians which can be seen in figure 2. Here the parameters are chosen to be $b_o = 2fm$ and $b_w 1.2fm$ as oscillator and interaction function should have an impact. These specific parameters are again chosen as they are successful when doing the optimisation.

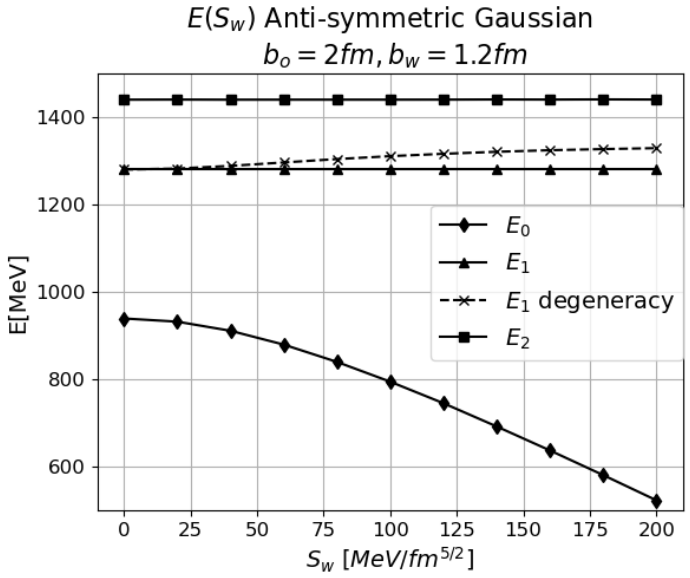

Figure 2: The energy levels as a function of S_w using an anti-symmetric Gaussian on the generalised eigenvalue problem. The parameters used are $b_o = 2fm$ and $b_w = 1.2fm$. Only one degeneracy is plotted for E_0 and E_2, while two are plotted for E_1, the remaining degeneracies can be found in appendix E.

Similarly to the system using symmetrical Gaussians, most degeneracies have been removed for simplicity. However, two degeneracies for E_1 have been kept as the one labelled E_1 *degeneracy* is the largest degeneracy. It is expected that at least some of the excited energy levels would decrease with an increase in S_w on approximately the same scale as the ground state does. As this is not the case it is a strong indication that ECGs confined with a harmonic oscillator potential cannot be used to determine the resonance of the system.

4.2 Varying b_o

To further determine if it is possible to use ECGs confined by a harmonic oscillator potential can be used to determine the mass of the Roper resonance, results are obtained with varying b_o. This is done for the non-relativistic system and $b_w = 1.42$ which proved to be a good parameter in [1]. Firstly S_w is chosen to be 27.4 as this is the same as in [1] when correcting for the $f(r)$ normalisation function used in the article. These results can be seen in figure 3.

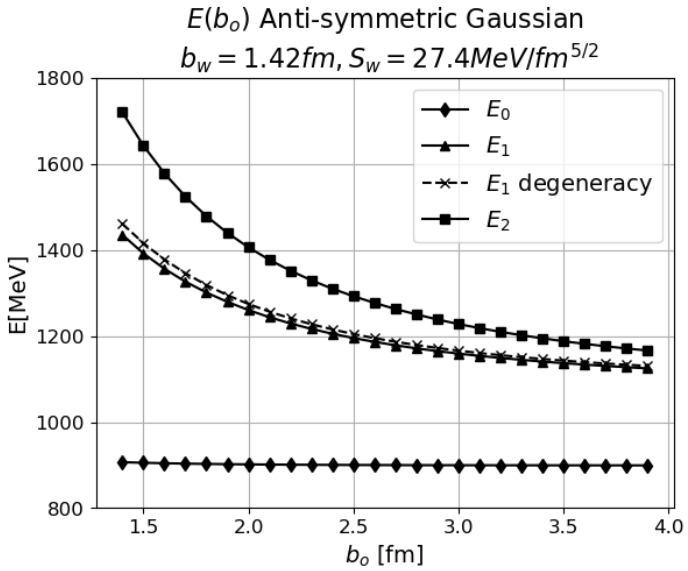

Figure 3: The energy levels as a function of b_o using $b_w = 1.42fm$ and $S_w = 27.4MeV/fm^{5/2}$. Only one degeneracy is plotted for E_0 and E_2, while two are plotted for E_1, the remaining degeneracies can be found in appendix E.

For the excited states at $S_w = 27.4$ the expected kink in the avoided crossings followed by a flattening of the graphs are not found. Only one state is shown for the second excited state while two degeneracies are shown for the first excited state as this is again the largest degeneary. The high degeneracy for E_1 matches the increasing degenerate state in fig 2. The full spectrum including all degenerate states can be found in appendix E.

As the relativistic correction is expected to be decrease the energy [14] the kink is expected to be higher than $1440MeV$. This can be artificially lowered

by increasing S_w. Thus, to ensure that the kink is not higher than the found energy states the same results are also found for $S_w = 80$ and $S_w = 180$. These results are quite similar, besides the ground state level, and can be seen in figure 4. As with figure 2 and 3 the same limited states are plotted. The full spectrums can be seen in appendix E.

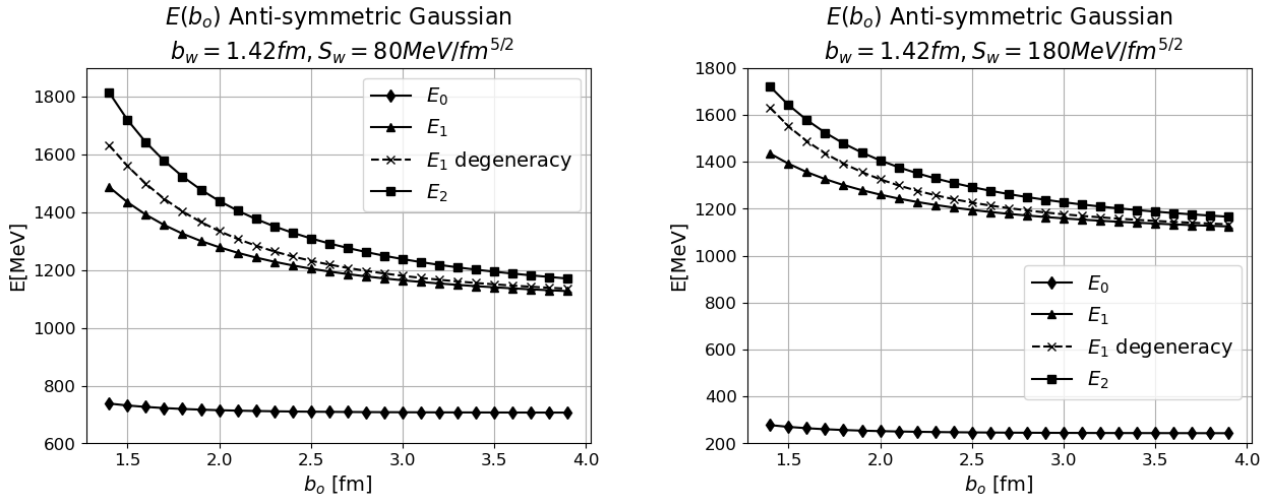

Figure 4: The energy levels as a function of b_o using $b_w = 1.42fm$ and $S_w = 80MeV/fm^{5/2}$ for the left and $b_w = 1.42fm$ and $S_w = 180MeV/fm^{5/2}$ for the right. Only one degeneracy is plotted for E_0 and E_2, while two are plotted for E_1, the remaining degeneracies can be found in appendix E.

The expected kink followed by a flattening is also not observed with the higher S_w. Therefore, this method cannot be used to determine the mass of the Roper resonance. And thus, the strength function will not be used as it would not provide good results.

4.3 Relativistic approach

The relativistic correction to the results is expected to decrease all energies by the same amount [14]. With this being the case, it does not make sense to obtain the relativistic results as these results would not be different than the non-relativistic results. Furthermore, good parameters which do not yield errors when trying to optimise are difficult to find for the relativistic case.

5 Discussion

The obtained results show that using ECGs confined by a harmonic oscillator potential cannot be used to determine the mass of the $N(1440)$ Roper resonance which also strongly indicates that the method cannot generally be used to determine the mass of larger particles. However, the reasoning behind this can still be discussed.

In general, the numerical calculations are very slow, even though the generalised eigenvalue problems are not very large. This is believed to mainly come from the fact that, the optimisation routine has problems finding the correct results, as the individual calculations are fairly quick. Furthermore, the optimisation routine will frequently have entrances in the matrices of the generalised eigenvalue problem which become NaN if the function parameters or initial optimisation parameters are bad. This problem is a further sign, that there are issues with the method, as all entrances of matrices yielded the expected results when using test-parameters. However, the use of Python combined with code that is not very well optimised will also have slowed down the calculations.

No more than the first two excited states are found for each calculation. This is due to the slow optimisation combined with a large degeneracy. Furthermore, not all the degenerate states are found for the second excited state, just the first four degeneracies which is enough to have an idea of where this state is and how it behaves. In addition to this, the NaN issues become more prevalent when increasing the size of the eigenvalue problem, thus making it even more advantageous to limit the size of the eigenvalue problem earlier than it would otherwise be preferred.

5.1 Varying S_w

While varying S_w the results using symmetric Gaussians were exactly as expected from equation 2.34, as the interaction overlaps are zero, due to the nature of the W ovelaps and symmetric Gaussians. This is a strong indication

of the script working.

For the anti-symmetric Gaussians, the results are also where they are expected for $S_w = 0$ when comparing to equation 2.33. When focusing on a smaller spectrum as in figure 5 the energies vary slightly, which indicates that the interaction overlap contributes to the energies even though they do not yield the expected results. However, the energy variation is not as expected, the energies are expected to follow a similar trend as the ground state. As the ground state behaves as expected it further confirms that the script works while the method does not.

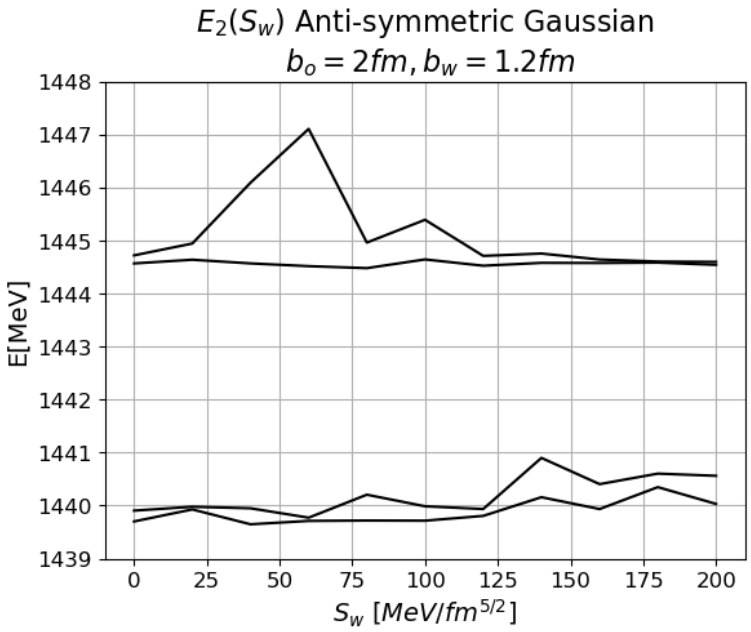

Figure 5: The four found degeneracies of second excited states using anti-symmetric Gaussians, varying S_w, $b_o = 2fm$, and $b_w = 1.2fm$. It can be observed that the energy levels do vary slightly when S_w changes, which indicates that the interaction function contributes to the energy. However, the energy levels are expected to decrease as S_w increases which is not the case.

The largest degeneracy found for the the first excited state in figure 2, while larger than the other degeneracies, which can be found in appendix E is not so large as to be problematic. This is due to the ground state having a much larger ΔE compared to this degeneary.

5.2 Varying b_o

When varying b_o the expected results are once again not found. However, after varying S_w and not getting good results it makes sense, that this could not provide good results. No new issues are found when varying b_o.

5.3 Relativistic approach

No results are obtained with relativistic kinetic energy. As mentioned earlier this is mainly due to the non-relativistic approach not yielding correct results. However, it is also partly due to issues with the numerical calculations when changing to the more complex calculations, as good parameters which does not yield errors are harder to find for the relativistic approach. This further indicates that the method is not feasible, either due to bad programming or simple because it does not work.

5.4 Change of method

If problems with the optimisation routine is the issue a fix could be to change the method to a one with a combined-physical state. In general, the approach is similar to everything done previous. However, instead of using four distinct physical state it could be changed to a combined physical state. This will decrease degeneracies of the system and thus decrease the size of the eigenvalue problem, which should make it easier to optimise for the individual levels. The reason this method is not used inititially is due to an increased complexity in the overlaps, which makes the initial calculation more difficult. Furthermore, the distinction between the proton and neutron, and π^0 and π^+ mass will be removed which means the exact mass can not be obtained through this method.

6 Conclusion

It has been shown that the mass of the $N(1440)$ Roper resonance cannot be determined using Explicitly Correlated Gaussians within the harmonic oscillator as the Artificial Confining Potential method. And it is thus highly unlikely that the method can be used to determine masses in more complex few-body systems.

References

[1] D. V. Fedorov. The N(1440) Roper resonance in the nuclear model with explicit mesons". *Few-Body Systems*, 65(32), 2024.

[2] Jim Mitroy, Sergiy Bubin, Wataru Horiuchi, Yasuyuki Suzuki, Ludwik Adamowicz, Wojciech Cencek, Krzysztof Szalewicz, Jacek Komasa, D. Blume, and Kálmán Varga. Theory and application of explicitly correlated Gaussians. *Rev. Mod. Phys.*, 85:693–749, May 2013.

[3] S. Navas et al. Review of Particle Physics. *Phys. Rev. D*, 110(3):030001, 2024.

[4] Francesco Terranova. *A Modern Primer in Particle and Nuclear Physics*. Oxford University Press, 11 2021.

[5] D. V. Fedorov. A Nuclear Model with Explicit Mesons. *Few-Body Systems*, 61(40), 2020.

[6] Y. Suzuki and K. Varga. *Stochastic variational approach to quantum-mechanical few body problems*, volume 54. 1998.

[7] David J. Griffiths and Darrell F. Schroeter. *Introduction to Quantum Mechanics*. Cambridge University Press, 3 edition, 2018.

[8] J. W. Verhoeven. Glossary of terms used in photochemistry (IUPAC Recommendations 1996). *Pure and Applied Chemistry*, 68(12):2223–2286, 1996.

[9] D. V. Fedorov, A. S. Jensen, M. Thøgersen, E. Garrido, and R. de Diego. Calculating Few-Body Resonances Using an Oscillator Trap. *Few-Body Systems*, 45(2):191–195, 2009.

[10] Francesco Giacosa, Anna Okopińska, and Vanamali Shastry. A simple alternative to the relativistic Breit–Wigner distribution. *The European Physical Journal A*, 57(12), December 2021.

[11] D. V. Fedorov. Analytic matrix elements with shifted correlated Gaussians. *Few-Body Systems*, 58(21), 2017.

[12] D. V. Fedorov. Private communications, 2026.

[13] D. V. Fedorov, A.F. Teilmann, M.C. Østerlund, and T.L. Norrbohm. Explicitly Correlated Gaussians with Tensor Pre-factors: Analytic Matrix Elements. *Few-Body Systems*, 65(75), 2024.

[14] A. I. Arbab. On relativistic harmonic oscillator. *Hadronic Journal*, 45(4):369–381, December 2022.

A Solutions to the sigma and tau overlaps

When calculating the results for $\langle S_1|\vec{\sigma}\vec{r}|S_2\rangle$ it is done by simple matrix calculations on the following identity:

$$\langle S_1|\vec{\sigma}\vec{r}|S_2\rangle = \langle S_1|\sigma_0|S_2\rangle\, r^0 + \sqrt{2}\,\langle S_1|\sigma_+|S_2\rangle\, r^- + \sqrt{2}\,\langle S_1|\sigma_-|S_2\rangle\, r^-. \tag{A.1}$$

Utilising:

$$\sigma_0 = \begin{pmatrix} 1 & 0 \\ 0 & -1 \end{pmatrix},\ \sigma_+ = \begin{pmatrix} 0 & 1 \\ 0 & 0 \end{pmatrix},\ \sigma_- = \begin{pmatrix} 0 & 0 \\ 1 & 0 \end{pmatrix}, \tag{A.2}$$

and $\uparrow = \begin{pmatrix} 1 \\ 0 \end{pmatrix}, \downarrow = \begin{pmatrix} 0 \\ 1 \end{pmatrix}$ results in the following:

$$\begin{aligned}
\langle\uparrow|\vec{\sigma}\vec{r}|\uparrow\rangle &= r^0, \\
\langle\uparrow|(\vec{\sigma}\vec{r})^\dagger|\uparrow\rangle &= r^0, \\
\langle\downarrow|\vec{\sigma}|\downarrow\rangle &= -r^0, \\
\langle\downarrow|(\vec{\sigma}\vec{r})^\dagger|\downarrow\rangle &= -r^0, \\
\langle\uparrow|\vec{\sigma}\vec{r}|\downarrow\rangle &= \sqrt{2}r^-, \\
\langle\uparrow|(\vec{\sigma}\vec{r})^\dagger|\downarrow\rangle &= \sqrt{2}r^+, \\
\langle\downarrow|\vec{\sigma}\vec{r}|\uparrow\rangle &= \sqrt{2}r^+, \\
\langle\downarrow|(\vec{\sigma}\vec{r})^\dagger|\uparrow\rangle &= \sqrt{2}r^-.
\end{aligned} \tag{A.3}$$

Similarly, the $\langle N_1\pi_1|\vec{\tau}\vec{\pi}|N_2\pi_2\rangle$ are found by matrix multiplication. However, in this case the known pion state is applied onto the $\vec{\tau}\vec{\pi}$ identity of:

$$\vec{\tau}\vec{\pi} = \tau_0\pi^0 + \sqrt{2}\tau_-\pi^+ + \sqrt{2}\tau_+\pi^-. \tag{A.4}$$

In this thesis there are only four different systems, being:

$$\langle p|\vec{\tau}\vec{\pi}|p\pi^0\rangle\,, \langle p|\vec{\tau}\vec{\pi}|n\pi^+\rangle\,, \langle p\pi^0|(\vec{\tau}\vec{\pi})^\dagger|p\rangle\,, \langle n\pi^+|(\vec{\tau}\vec{\pi})^\dagger|p\rangle\,. \tag{A.5}$$

Using $p = \begin{pmatrix} 1 \\ 0 \end{pmatrix}, n = \begin{pmatrix} 0 \\ 1 \end{pmatrix}$ the results are:

$$\begin{aligned} \langle p|\vec{\tau}\vec{\pi}|p\pi^0\rangle &= 1, \\ \langle p|\vec{\tau}\vec{\pi}|n\pi^+\rangle &= \sqrt{2}, \\ \langle p\pi^0|(\vec{\tau}\vec{\pi})^\dagger|p\rangle &= 1, \\ \langle n\pi^+|(\vec{\tau}\vec{\pi})^\dagger|p\rangle &= \sqrt{2}. \end{aligned} \tag{A.6}$$

B Analytical calculation of harmonic oscillator potential integral

The integral $I = \int_{-\infty}^{\infty} e^{-\alpha r^2 + \vec{\beta}\cdot\vec{r}} r^2 \, d^3r$ can be calculated analytically by substitution, which is done as follows:

Firstly, the exponent is rewritten such that:

$$-\alpha r^2 + \vec{\beta}\cdot\vec{r} = -\alpha\left(\vec{r} - \frac{\vec{\beta}}{2\alpha}\right)^2 + \frac{\beta^2}{4\alpha}. \tag{B.1}$$

Thus, making the integral:

$$I = e^{\frac{\beta^2}{4\alpha}} \int_{-\infty}^{\infty} e^{-\alpha\left(\vec{r} - \frac{\vec{\beta}}{2\alpha}\right)^2} r^2 \, d^3r. \tag{B.2}$$

Now a substitution of $\vec{u} = \vec{r} - \frac{\vec{\beta}}{2\alpha}$ is made which implies $\frac{d\vec{u}}{d\vec{r}} = 1 \implies d^3u = d^3r$. Furthermore, $\vec{r} = \vec{u} + \frac{\vec{\beta}}{2\alpha}$ and therefore, $r^2 = |\vec{u} + \frac{\vec{\beta}}{2\alpha}|^2 = u^2 + \frac{\beta^2}{4\alpha^2} + 2\vec{u}\cdot\frac{\vec{\beta}}{2\alpha}$. The limits of the integral do not change by this substitution. If this is applied to the integral it yields:

$$I = e^{\frac{\beta^2}{4\alpha}} \int_{-\infty}^{\infty} e^{-\alpha u^2} \left(u^2 + \frac{\beta^2}{4\alpha^2} + 2\vec{u}\cdot\frac{\vec{\beta}}{2\alpha}\right) d^3u. \tag{B.3}$$

The last term here is 0 as it is an odd integrand over a symmetric integral. Thus, the integral becomes:

$$I = e^{\frac{\beta^2}{4\alpha}} \left(\int_{-\infty}^{\infty} e^{-\alpha u^2} u^2 \, d^3u + \int_{-\infty}^{\infty} e^{-\alpha u^2} \frac{\beta^2}{4\alpha^2} d^3u\right). \tag{B.4}$$

Converting these to standard spherical integrals they become standard Gaussian integrals with well-known solutions [7]. Thus, the integral becomes:

$$
\begin{aligned}
I &= e^{\frac{\beta^2}{4\alpha}} \left(4\pi \int_0^\infty e^{-\alpha u^2} u^4 \, du + 4\pi \int_0^\infty e^{-\alpha u^2} \frac{\beta^2}{4\alpha^2} u^2 \, du \right) \\
&= e^{\frac{\beta^2}{4\alpha}} \left(4\pi \frac{3\sqrt{\pi}}{8\alpha^{5/2}} + 4\pi \frac{\beta^2}{4\alpha^2} \frac{\sqrt{\pi}}{4\alpha^{3/2}} \right) \\
&= e^{\frac{\beta^2}{4\alpha}} \left(\frac{\pi}{\alpha} \right)^{3/2} \left(\frac{\beta^2}{4\alpha^2} + \frac{3}{2\alpha} \right).
\end{aligned}
\tag{B.5}
$$

C Analytical calculation of strength function integral

When it comes to the strength function integral $J = \int_{-\infty}^{\infty} e^{-\alpha r^2+\vec{\beta}\cdot\vec{r}}\frac{1}{r}d^3r$ the result is found by first utilising that $\vec{\beta}\cdot\vec{r}$ can be written as $\beta r\cos(\theta)$, thus rewriting the integral to be:

$$\begin{aligned} J = \int_{-\infty}^{\infty} e^{-\alpha r^2+\vec{\beta}\cdot\vec{r}}\frac{1}{r}d^3r = \int_0^{\infty}\int_0^{\pi}\int_0^{2\pi} e^{-\alpha r^2+\beta r\cos(\theta)}\frac{1}{r}r^2\sin(\theta)\,d\phi\,d\theta\,dr \\ = 2\pi\int_0^{\infty} e^{-\alpha r^2} r\int_0^{\pi} e^{\beta r\cos(\theta)}\sin(\theta)\,d\theta\,dr. \end{aligned} \tag{C.1}$$

The angular integral is solved by substitution of $o = \cos(\theta)$, thus $\frac{do}{d\theta} = -\sin(\theta) \implies d\theta = -\frac{do}{\sin(\theta)}$. The limits of the integral will also change as $\cos(0) = 1, \cos(\pi) = -1$. Then the angular integral is:

$$\begin{aligned} \int_0^{2\pi} e^{\beta r\cos(\theta)}\sin(\theta)\,d\theta = \int_1^{-1} e^{\beta ro}\sin(\theta)\frac{-1}{\sin(\theta)}\,do = \int_{-1}^{1} e^{\beta ro}\,do \\ = \left[\frac{e^{\beta ro}}{\beta r}\right]_{o=-1}^{o=1} = \frac{e^{\beta r}-e^{-\beta r}}{\beta r}. \end{aligned} \tag{C.2}$$

This gives the following integral to calculate:

$$\begin{aligned} J = 2\pi\int_0^{\infty} e^{-\alpha r^2}\frac{e^{\beta r}-e^{-\beta r}}{\beta}\,dr \\ \frac{2\pi}{\beta}\int_0^{\infty} e^{-\alpha r^2+\beta r}\,dr - \frac{2\pi}{\beta}\int_0^{\infty} e^{-\alpha r^2-\beta r}\,dr = \frac{2\pi}{\beta}(I_+ - I_-). \end{aligned} \tag{C.3}$$

To calculate this integral the error function is used, with the known identity:

$$\frac{2}{\sqrt{\pi}}\int_z^{\infty} e^{-t^2}\,dt = 1 - \frac{2}{\sqrt{\pi}}\int_0^{z} e^{-t^2}\,dt = 1 - \mathrm{erf}(z). \tag{C.4}$$

The integrals are calculated as such:

$$\begin{aligned} I+ = \int_0^\infty e^{-\alpha r^2+\beta r}\,dr &= \int_0^\infty e^{-\alpha\left(r-\frac{\beta}{2\alpha}\right)^2+\frac{\beta^2}{4\alpha}}\,dr = e^{\frac{\beta^2}{4\alpha}}\int_0^\infty e^{-\alpha\left(r-\frac{\beta}{2\alpha}\right)^2}\,dr \\ &= e^{\frac{\beta^2}{4\alpha}}\int_{-\frac{\beta}{2\sqrt{\alpha}}}^\infty e^{-u^2}\frac{1}{\sqrt{\alpha}}\,du = e^{\frac{\beta^2}{4\alpha}}\frac{\sqrt{\pi}}{2\sqrt{\alpha}}(1-\operatorname{erf}(-\frac{\beta}{2\sqrt{\alpha}})), \end{aligned} \tag{C.5}$$

$$\begin{aligned} I- \int_0^\infty e^{-\alpha r^2-\beta r}\,dr &= \int_0^\infty e^{-\alpha\left(r+\frac{\beta}{2\alpha}\right)^2+\frac{\beta^2}{4\alpha}}\,dr = e^{\frac{\beta^2}{4\alpha}}\int_0^\infty e^{-\alpha\left(r+\frac{\beta}{2\alpha}\right)^2}\,dr \\ &= e^{\frac{\beta^2}{4\alpha}}\int_{\frac{\beta}{2\sqrt{\alpha}}}^\infty e^{-k^2}\frac{1}{\sqrt{\alpha}}\,dk = e^{\frac{\beta^2}{4\alpha}}\frac{\sqrt{\pi}}{2\sqrt{\alpha}}(1-\operatorname{erf}(\frac{\beta}{2\sqrt{\alpha}})). \end{aligned} \tag{C.6}$$

Before adding the two integrals the following identity is used:

$$\operatorname{erf}(-z) = -\operatorname{erf}(z). \tag{C.7}$$

Thus, resulting in:

$$\begin{aligned} J = \frac{2\pi}{\beta}e^{\frac{\beta^2}{4\alpha}}\frac{\sqrt{\pi}}{2\sqrt{\alpha}}(1+\operatorname{erf}(\frac{\beta}{2\sqrt{\alpha}}) - (1-\operatorname{erf}(\frac{\beta}{2\sqrt{\alpha}}))) \\ = e^{\frac{\beta^2}{4\alpha}}\frac{2\pi^{3/2}}{\alpha}\operatorname{erf}(\frac{\beta}{2\sqrt{\alpha}}). \end{aligned} \tag{C.8}$$

The error function integral can be calculated numerically.

D Numerical methods

The numerical results are obtained using Python and the optimisation is done through the SciPy package. The L-BFGS-B method is chosen as the optimisation method due to its speed and the ability to customise a wide array of options.

The optimisation is done by first constructing four Gaussians with different spin-isospin states, these are used to optimise for the ground state. The initial optimisation parameters are chosen to be close to the expected values. Then four more Gaussians with four different spin-isospin states are added. These can be used to either optimise for one eigenvalue or a sum of eigenvalue. While debugging it was mainly one eigenvalue was used, when finished it should optimise for multiple eigenvalues at a time. More Gaussians are added to get more states and so forth.

When doing the numerical calculations, the matrix as described in eq. 2.35 is built without the anti-symmetrisation. The goal is then to debug for a symmetric non-relativistic system with no interaction function ($S_w = 0$)[3]. Then the goal is to use the anti-symmetric approach. This is done first, as the solutions to these systems are well known. After the non-relativistic results are correct it is repeated with relativistic kinetic energies. If this proves to work, the steps should be repeated with a low powered interaction function ($S_w \approx 1MeV$). Then it can be repeated with varying S_w from which a lowering of the energies is expected with the anti-symmetrical Gaussians.

After the initial calculations are shown to be correct the b_o values can be altered. As the b_o values are only altered slightly, for each step the optimisation process can be sped up by using the previously found parameters as new initial optimisation parameters.

Lastly if the previous steps are shown to work the strength function with the Breit-Wigner fit can be used to determine the resonance and width.

[3]This system is slightly simpler and therefore used first, it has a general solution of $E_n^{symmmetric} = \hbar\omega(2n + \frac{3}{2})$.

E Plots with all degenerate states

The figures in this appendix show all the degenerate states of the found energy spectrums.

E.1 S_w as a parameter

E.1.1 The symmetric Gaussian

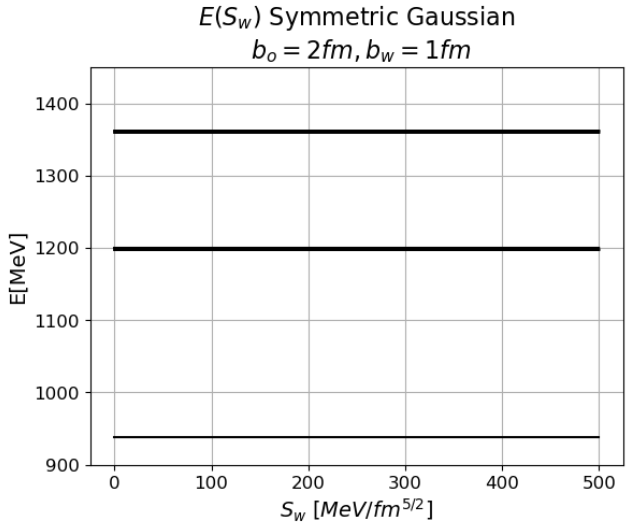

Figure 6: The full energy spectrum for the symmetric Gaussian with S_w as a parameter and $b_o = 2$, $b_w = 1.2$.

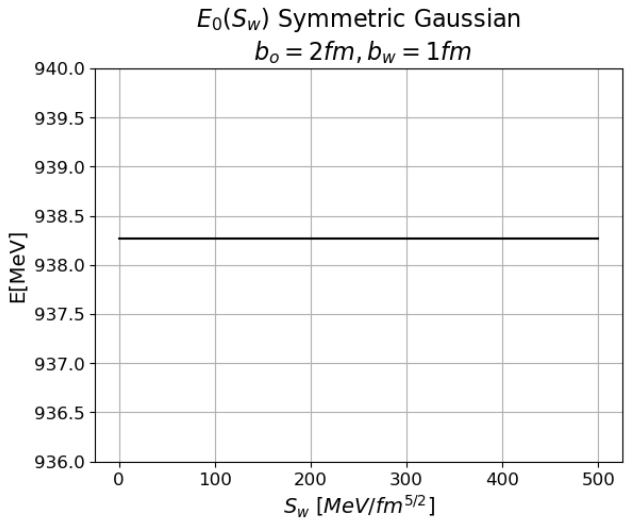

Figure 7: The energy spectrum for the symmetric Gaussian with S_w as a parameter and $b_o = 2$, $b_w = 1.2$. Zoomed to between 936 and 940 MeV.

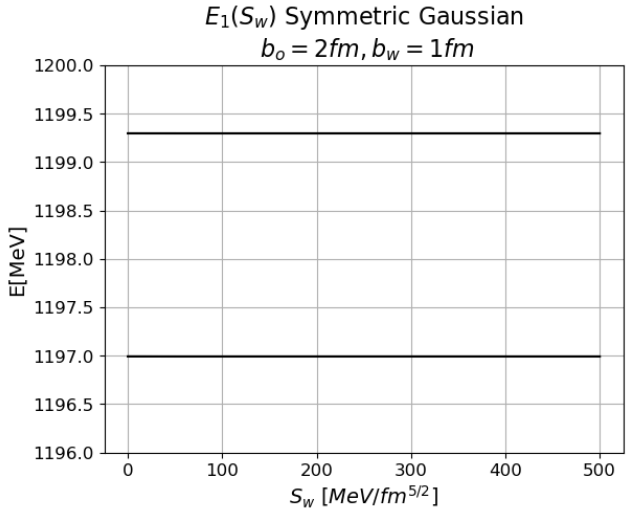

Figure 8: The energy spectrum for the symmetric Gaussian with S_w as a parameter and $b_o = 2$, $b_w = 1.2$. Zoomed to between 1196 and 1200 MeV. For each of the two visible states there are further two degenerate states, however they are so close that they are indistinguishable.

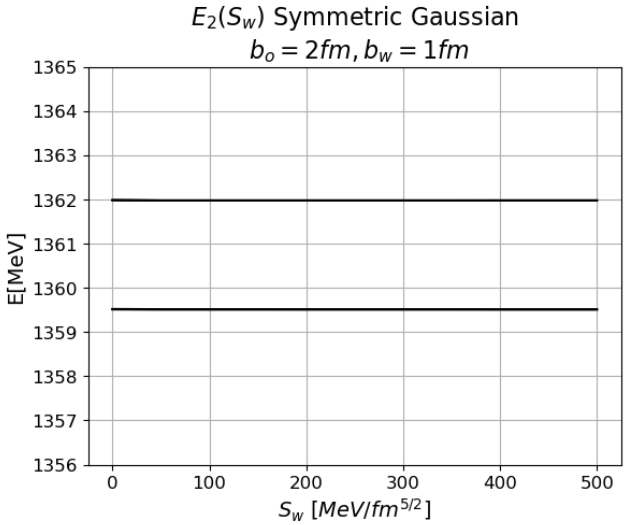

Figure 9: The energy spectrum for the symmetric Gaussian with S_w as a parameter and $b_o = 2$, $b_w = 1.2$. Zoomed to between 1365 and 1365 MeV. For each of the two visible states there are further two degenerate states, however they are so close that they are indistinguishable.

E.1.2 The anti-symmetric Gaussian

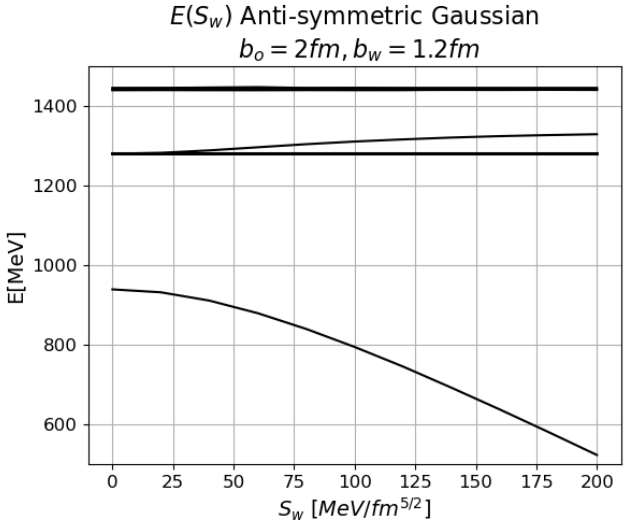

Figure 10: The full energy spectrum for the anti-symmetric Gaussian with S_w as a parameter and $b_o = 2$, $b_w = 1.2$.

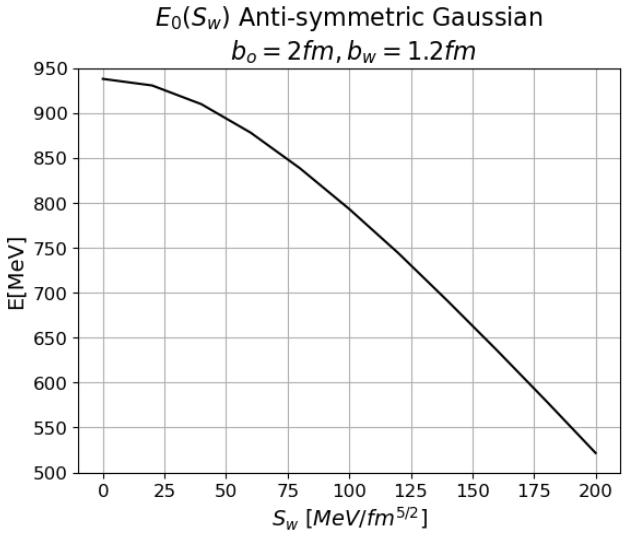

Figure 11: The energy spectrum for the anti-symmetric Gaussian with S_w as a parameter and $b_o = 2$, $b_w = 1.2$. Zoomed to between 500 and 950 MeV.

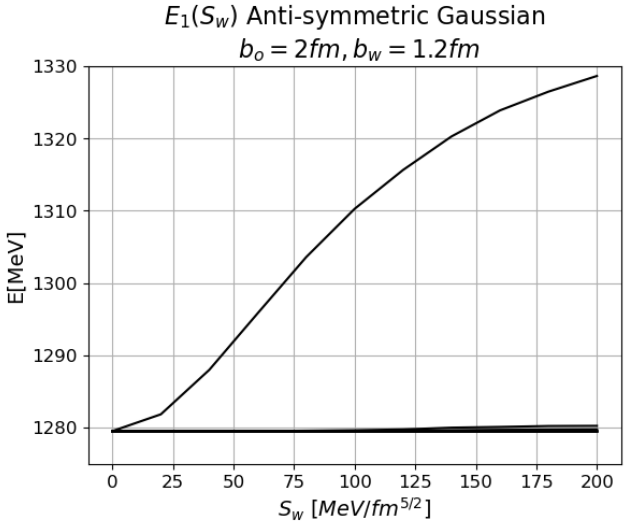

Figure 12: The energy spectrum for the anti-symmetric Gaussian with S_w as a parameter and $b_o = 2$, $b_w = 1.2$. Zoomed to between 1275 and 1330 MeV. 12 degenerate states are plotted here, however most of them are indistinguishable due to the low energy difference.

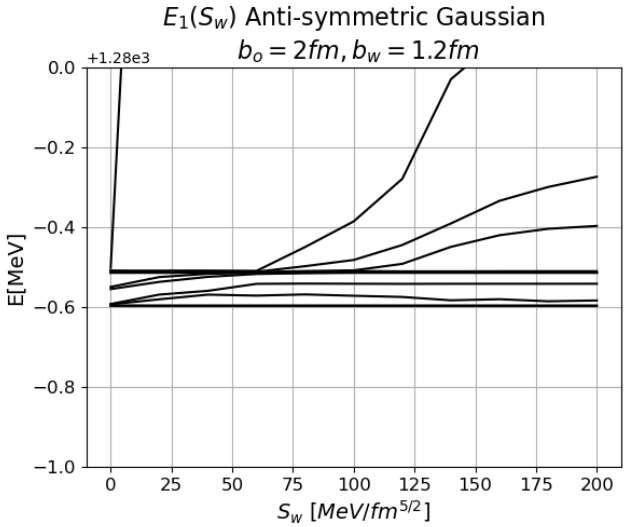

Figure 13: The energy spectrum for the anti-symmetric Gaussian with S_w as a parameter and $b_o = 2$, $b_w = 1.2$. Zoomed to between 1279 and 1280 MeV. 12 degenerate states are plotted here, however some of them are indistinguishable due to the low energy difference.

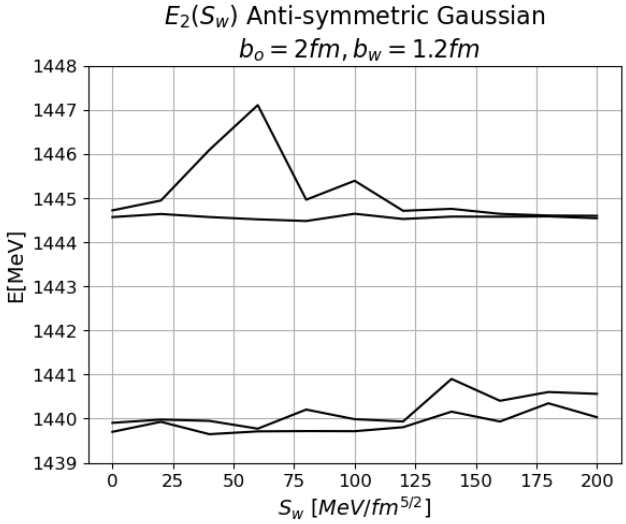

Figure 14: The energy spectrum for the anti-symmetric Gaussian with S_w as a parameter and $b_o = 2$, $b_w = 1.2$. Zoomed to between 1439 and 1448 MeV.

E.2 b_o as the parameter

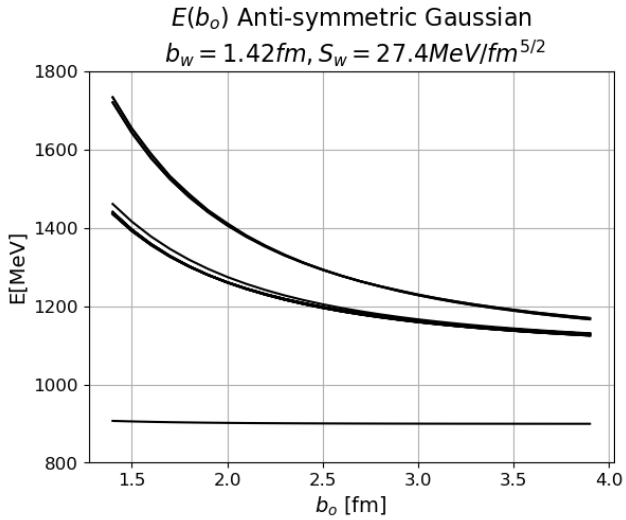

Figure 15: The full energy spectrum with b_o as a parameter and $b_w = 1.42$, $S_w = 27.4$. For E_1 (the energies starting at ≈ 1400 MeV) there are twelve degeneracies with most of them being indistinguishable due to their proximity. For E_2 (the energies starting at ≈ 1750 MeV) there are four found degeneracies.

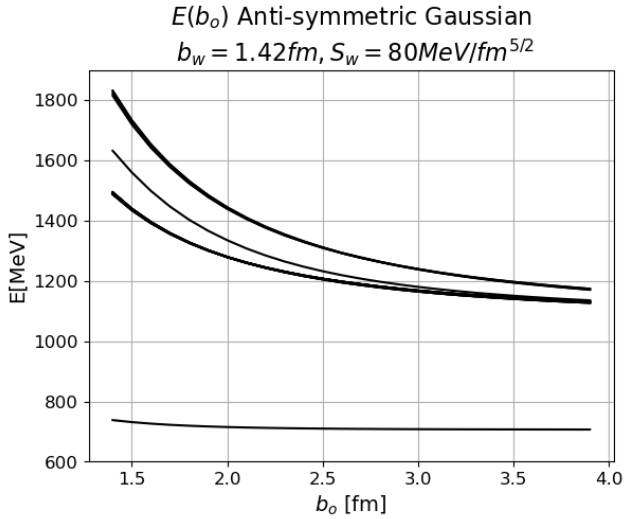

Figure 16: The full energy spectrum with b_o as a parameter and $b_w = 1.42$, $S_w = 80$. For E_1 (the energies starting at ≈ 1500 and ≈ 1600 MeV) there are twelve degeneracies with most of them being indistinguishable due to their proximity. For E_2 (the energies starting at ≈ 1800 MeV) there are four found degeneracies.

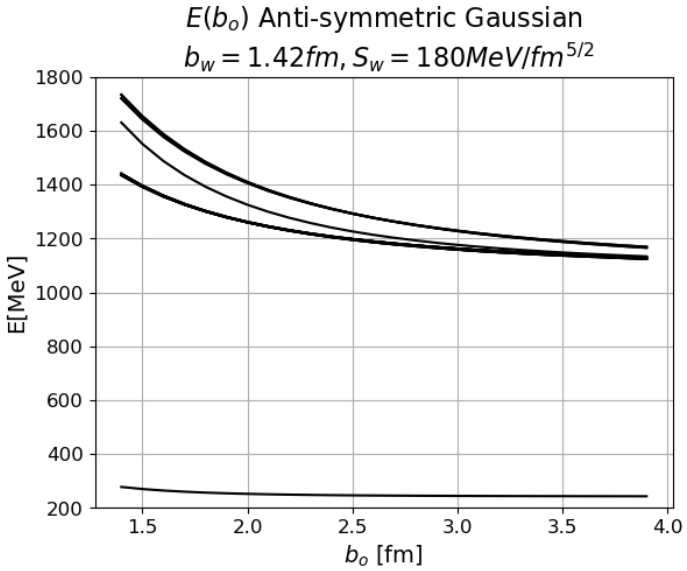

Figure 17: The full energy spectrum with b_o as a parameter and $b_w = 1.42$, $S_w = 180$. For E_1 (the energies starting at ≈ 1450 and ≈ 1650 MeV) there are twelve degeneracies with most of them being indistinguishable due to their proximity. For E_2 (the energies starting at ≈ 1700 MeV) there are four found degeneracies.

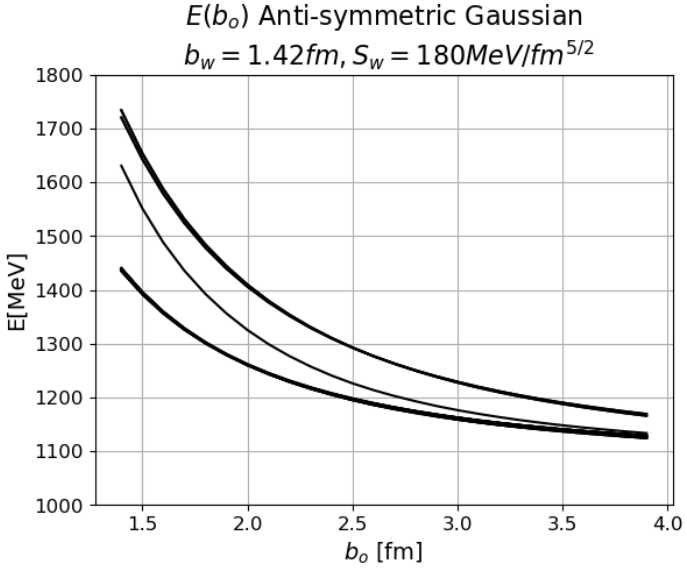

Figure 18: The energy spectrum with b_o as a parameter and $b_w = 1.42$, $S_w = 180$. Zoomed to between 1000 and 1800 MeV.For E_1 (the energies starting at ≈ 1450 and ≈ 1650 MeV) there are twelve degeneracies with most of them being indistinguishable due to their proximity. For E_2 (the energies starting at ≈ 1700 MeV) there are four found degeneracies.